Title
General Synthetic Approach to Diverse Taxane Cores

Journal
Journal of the American Chemical Society, 144(46)

ISSN
0002-7863

Authors
Perea, Melecio A
Wang, Brian
Wyler, Benjamin C
et al.

Publication Date
2022-11-23

DOI
10.1021/jacs.2c10272

Peer reviewed

HHS Public Access

Author manuscript

J Am Chem Soc. Author manuscript; available in PMC 2023 February 06.

Published in final edited form as:

J Am Chem Soc. 2022 November 23; 144(46): 21398–21407. doi:10.1021/jacs.2c10272.

General Synthetic Approach to Diverse Taxane Cores

Melecio A. Perea[†],
Department of Chemistry, University of California, Berkeley, California 94720, United States

Brian Wang[†],
Department of Chemistry, University of California, Berkeley, California 94720, United States

Benjamin C. Wyler,
Department of Chemistry, University of California, Berkeley, California 94720, United States

Jin Su Ham,
Department of Chemistry, University of California, Berkeley, California 94720, United States

Nicholas R. O'Connor,
Department of Chemistry, University of California, Berkeley, California 94720, United States

Shota Nagasawa,
Department of Chemistry, University of California, Berkeley, California 94720, United States

Yuto Kimura,
Department of Chemistry, University of California, Berkeley, California 94720, United States

Carolin Manske,
Department of Chemistry, University of California, Berkeley, California 94720, United States

Maximilian Scherübl,
Department of Chemistry, University of California, Berkeley, California 94720, United States

Johny M. Nguyen,
Department of Chemistry, University of California, Berkeley, California 94720, United States

Richmond Sarpong
Department of Chemistry, University of California, Berkeley, California 94720, United States

Abstract

Corresponding Author: **Richmond Sarpong** – *Department of Chemistry, University of California, Berkeley, California 94720, United States;* rsarpong@berkeley.edu.

[†]Author Contributions

M.A.P. and B.W. contributed equally.

Supporting Information

The Supporting Information is available free of charge at https://pubs.acs.org/doi/10.1021/jacs.2c10272.

Experimental procedures, characterization data, NMR spectra, and X-ray crystallographic data (PDF)

Accession Codes

CCDC 2178150–2178154 contain the supplementary crystallographic data for this paper. These data can be obtained free of charge via www.ccdc.cam.ac.uk/data_request/cif, or by emailing data_request@ccdc.cam.ac.uk, or by contacting The Cambridge Crystallographic Data Centre, 12 Union Road, Cambridge CB2 1EZ, UK; fax: +44 1223 336033.

The authors declare no competing financial interest.

Complete contact information is available at: https://pubs.acs.org/10.1021/jacs.2c10272

Chemical synthesis of natural products is typically inspired by the structure and function of a target molecule. When both factors are of interest, such as in the case of taxane diterpenoids, a synthesis can both serve as a platform for synthetic strategy development and enable new biological exploration. Guided by this paradigm, we present here a unified enantiospecific approach to diverse taxane cores from the feedstock monoterpenoid (*S*)-carvone. Key to the success of our approach was the use of a skeletal remodeling strategy which began with the divergent reorganization and convergent coupling of two carvone-derived fragments, facilitated by Pd-catalyzed C–C bond cleavage tactics. This coupling was followed by additional restructuring using a Sm(II)-mediated rearrangement and a bioinspired, visible-light induced, transannular [2 + 2] photocycloaddition. Overall, this divergent monoterpenoid remodeling/convergent fragment coupling approach to complex diterpenoid synthesis provides access to structurally disparate taxane cores which have set the stage for the preparation of a wide range of taxanes.

Graphical Abstract

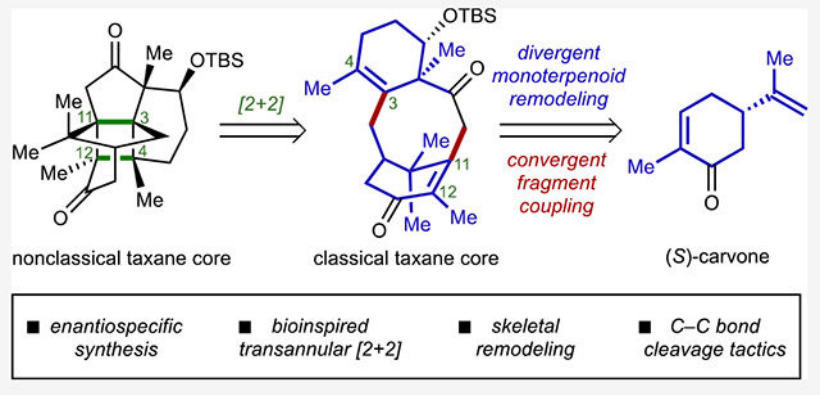

INTRODUCTION

Taxane natural products (representative examples shown in Figure 1) make up a large, diverse collection of diterpenoids (>500 members isolated to date).[1] These secondary metabolites exhibit significant anticancer properties[2,3] and account for some of the most topologically complex diterpenoid frameworks found in nature. On the basis of their structures, taxanes can be generally categorized as either classical or nonclassical.[4] Classical taxanes (e.g., **1–3**, Figure 1A) feature a 6/8/6 ring system decorated with unique oxygenation patterns, while nonclassical taxanes contain modifications to these functionalized 6/8/6 cores, such as additional transannular bonds (e.g., cyclotaxanes **4–6**, Figure 1B). Biosynthetically, taxanes arise from geranylgeranyl diphosphate (GGPP, **7**, Figure 1C), which first undergoes a series of stereoselective cyclizations to assemble the A, B, and C rings of the classical taxane system (**8**). It is proposed that oxidized variants of this core can then undergo transannular bond formations, such as an intramolecular aldol and transannular [2 + 2] cycloaddition, to construct nonclassical cyclotaxane frameworks (e.g., **9**).[1]

Owing to their remarkable bioactivity profiles and intricate architectures, taxanes have long served as a source of inspiration and creativity for medicinal and synthetic chemists. For

example, taxol (**1**), the flagship member of the family due to its clinical relevance as a potent chemotherapeutic, has inspired a total of twelve chemical syntheses.[5–19] Recently, the Baran group disclosed a series of publications outlining their "two-phase approach" to taxane synthesis, which combined a cyclase phase (a series of ring-forming events) with an oxidase phase (an orchestrated oxidation sequence) to provide access to taxol (**1**) as well as other taxol-like congeners.[17] However, aside from **1** and its closely related congeners, the vast majority of taxane chemical space remains underexplored. To date, there has only been one synthesis of a nonclassical cyclotaxane, canataxpropellane (**4**), which was achieved by Gaich and co-workers in 2020 in an elegant and expedient fashion.[20] Overall, this scarcity of structurally diverse taxane syntheses can be attributed, in part, to the added synthetic challenges associated with accessing congeners that vary significantly in structure. For example, syntheses of taxagifine (**2**) and taxezopidine A (**3**) would require the installation of additional C17–C12 and C17–C13 oxo-bridges, while preparation of canataxpropellane (**4**), taxpropellane (**5**), and taxinine K (**6**) would all require the construction of highly caged skeletons.

Despite its effectiveness in the clinical setting, taxol-based therapy often encounters critical challenges, including diminished efficacy due to the emergence of drug-resistant cancer cells.[21–23] Such a challenge underscores the necessity for accessing unique taxane chemical space in order to comprehensively evaluate the bioactivities of diverse congeners, like **2–6**, and identify next-generation anticancer agents.[24] In fact, developing one chemical synthesis approach to both classical and nonclassical taxanes would greatly streamline these efforts; however, such a feat has remained elusive due to the vast structural diversity and complexity of these molecules. Inspired by the challenge of developing a general solution for their preparation, we set out to design a strategy that would enable unified enantiospecific access to structurally diverse taxanes. This Article discusses the first stage of our plan, akin to the cyclase phase of the Baran approach,[17,25] in which we employ a skeletal remodeling strategy, enabled by bond cleavage tactics, to reorganize two monoterpenoid (in this case, carvone) units into diverse taxane diterpenoid cores designed strategically to facilitate downstream oxidations and diversification.

Strategy Design.

Our research group has had a longstanding interest in developing and applying skeletal remodeling strategies to transform "chiral pool" terpenes[26]—enantioenriched feedstocks—into diverse natural product-like scaffolds.[27–29] Recently, we demonstrated how C–C bond cleavage, powered by rhodium and palladium catalysis, can be used to remodel both enantiomeric forms of the feedstock terpenoid carvone (**10** and *ent*-**10**, Figure 2A) into diverse diterpenoid natural products, including phomactin A[30] and xishacorene B.[31] Specifically, our strategy focused on leveraging known cyclobutanols (**11**, **12**, *ent*-**11**, and *ent*-**12**)[32]—formed as diastereomeric pairs from carvone—in transition metal-catalyzed C–C bond cleavage reactions.[33] For both the phomactins and xishacorene B, the diterpenoid frameworks were assembled by coupling only one diastereomer of the carvone-derived cyclobutanols (i.e., **12** for the phomactins and *ent*-**11** for xishacorene B) with non-terpenoid units containing the requisite number of carbons to complete the skeleton. Furthermore, in a preliminary investigation inspired by the early work of Uemura and co-workers,[34]

we applied a Pd(0)-catalyzed C–C bond cleavage/cross-coupling reaction to remodel cyclobutanol **12** to a simplified taxagifine core.[28] Despite laying the foundation for the work discussed herein, the synthesis of **12** produced a scaffold lacking both crucial stereochemical information in the C-ring as well as a key oxidation at the C13 position. As a result of these two factors, this scaffold could not be advanced productively. We sought to address these limitations and ultimately expand upon our entire carvone remodeling paradigm by using not just one but both diastereomeric cyclobutanols in a unified synthesis of taxanes. Specifically, we hypothesized that by using Pd-catalyzed C–C bond cleavage tactics, these two carvone-derived fragments, each representing a monoterpenoid unit, could undergo divergent remodeling/convergent fragment coupling to forge the entire diterpenoid network of the taxane architecture, thus demonstrating a novel approach to complex diterpenoid synthesis.

Guided by our goal of accessing diverse taxanes, we envisioned that both nonclassical (**13**, Figure 2B) and classical (**14–16**) frameworks could be assembled from (*S*)-carvone (**10**) by merging bioinspired logic with modern skeletal remodeling tools. Retrosynthetically, we proposed that the nonclassical cyclotaxane core (**13**) would arise from taxol core **14**, a classical taxane framework, which in the forward sense would undergo a bioinspired transannular [2 + 2] photocycloaddition between the electronically matched C3–C4 and C11–C12 alkene groups. Preliminary computations used to visualize the conformation of **14** revealed the two alkenes to be well-aligned and in close proximity, thus supporting our proposal (Supporting Information, page S26). Taxol core **14** was envisioned to arise from the taxezopidine A core (**15**), which, in turn, would be obtained from the taxagifine core (**16**) through remodeling of the A-ring. Specifically, we envisioned that reduction of the C13 carbonyl of **16** with a one-electron donor (e.g., SmI_2) would facilitate rearrangement to **15** by effecting fragmentation of the C12–O bond followed by formation of the C13–O bond.[35] A C17 deoxygenation would then provide the taxol core (**14**). Importantly, these cores all contain pre-installed functionality that could be leveraged in the future for executing the remaining C2, C5, and C10 oxidations. For example, in the classical taxane cores, both the C2 and C5 positions are adjacent to an alkene that could enable allylic oxidations, and the C10 position could be functionalized through an enolate oxidation. Elaboration of the nonclassical cyclotaxane core (**13**) to the corresponding target natural products (i.e., **4** and **5**) would require remote C–H oxidations; however, the pre-installed oxygen functionality in **13** could potentially be applied in a redox-relay approach[36] or a directed C–H oxidation strategy.[37] Alternatively, performing the transannular [2 + 2] cycloaddition on a derivative of taxol core **14** bearing all the requisite oxygenation could achieve the same net result. The taxagifine core (**16**) was envisioned to arise from two fragments, a C-ring fragment (**17**) and an A-ring fragment (**18**), which in the forward sense would be joined together through a tandem C–C bond cleavage/cross-coupling reaction followed by an intramolecular aldol cyclization to forge the B-ring. Notably, these fragments contain five out of the eight oxygen functional groups present on the fully oxidized taxagifine system, thus limiting the need for late-stage oxidations—a potentially challenging task on complex scaffolds.[38] Finally, the C- and A-ring fragments would arise from diastereomeric cyclobutanols **11** (major diastereomer) and **12** (minor diastereomer) which would simultaneously be obtained

from (*S*)-carvone (**10**) through an epoxidation/Ti(III)-mediated cyclization sequence[32] in the forward sense.

RESULTS AND DISCUSSION

Synthesis of the Coupling Fragments.

We began our studies with the synthesis of the C-ring fragment (**17**, Figure 3A) from the major cyclobutanol diastereomer (**11**), which was obtained from (*S*)-carvone following a known two step procedure[32] involving epoxidation of the isopropenyl moiety on carvone followed by a Ti(III)-mediated epoxide-ring opening/radical cyclization into the carbonyl group (Supporting Information, page S5). Protection of the primary hydroxy group in **11** gave the TBS-protected major cyclobutanol (**19**), which subsequently underwent a Pd(II)-catalyzed cleavage of the less substituted C–C bond followed by *β*-hydride elimination to afford cyclohexenone **20**.[39] A 1,4-reduction of the enone with L-selectride provided **21** as an inconsequential mixture of diastereomers that were both converted to vinyl triflate **22** upon treatment with KHMDS and $PhNTf_2$. The exo-methylene of **22** was then oxidatively cleaved to afford the corresponding ketone (**23**) using the Lemieux–Johnson[40] protocol with 2,6-lutidine[41] as an additive. Next, unveiling of the primary hydroxy group following TBS cleavage provided keto-alcohol **24**. By leveraging the directing ability of this hydroxy group, an Evans–Saksena[42,43] reduction of the ketone with $Me_4N(OAc)_3BH$ was performed to obtain diol **25**. Finally, a one-pot TEMPO/PIDA oxidation[44] of the primary hydroxy group and TBS-protection of the secondary hydroxy group afforded the completed C-ring fragment (**17**).

The synthesis of the A-ring fragment (**18**, Figure 3B) began with an oxidative cyclization sequence in which *m*-CPBA epoxidation of the minor cyclobutanol diastereomer (**12**) promoted a cyclization of the primary hydroxy group to the C12 position, thus affording diol **26**.[27] Notably, this sequence constructed the key C17–C12 oxo-bridge of the taxagifine scaffold (**16**), while simultaneously installing the C13 oxygenation present in taxanes **1**–**6**. Next, the C13 hydroxy group of diol **26** was oxidized to the corresponding ketone using Dess–Martin periodinane (DMP)[45] to afford keto-alcohol **27**. Subjecting this intermediate to Noyori ketalization[46] conditions gave a mixture of the desired A-ring fragment (**18**) and a derivative with the tertiary hydroxy group protected as the trimethylsilyl (TMS) ether (not shown). Deprotection of this TMS-protected A-ring fragment with TBAF (Supporting Information, page S12) provided **18** in 64% yield over two steps. With both coupling fragments now in hand, we shifted our attention to investigating the key C–C bond cleavage/cross-coupling reaction.

Development of the C–C Bond Cleavage/Cross-Coupling.

While our previous studies had demonstrated that a Pd-catalyzed C–C bond cleavage/cross-coupling between a carvone-derived cydobutanol and an aryl bromide could provide a simplified taxagifine-like scaffold[28] (Figure 2A), the success of our new unified synthetic route would ultimately hinge upon extending this convergent strategy to more complex and highly functionalized coupling partners (i.e., **17** and **18**). Evaluation of reaction conditions began by using $Pd(OAc)_2$ as the pre-catalyst, SPhos as the ligand, Cs_2CO_3 as the base, and

benzene as the solvent (entry 1, Figure 4A). Under these conditions, we did not observe any of the desired cross-coupled product (**28**), but instead obtained an undesired diastereomer (**29**) of the cross-coupled adduct in 30% yield, with unexpected stereoinversion occurring at the C1 position. Mechanistically, the desired coupling product (**28**) was envisioned to arise from oxidative addition of an in situ generated Pd(0) catalyst into the vinyl triflate group of **17** to give Pd(II)-intermediate **30** (Figure 4B). This complex would then undergo ligand exchange with cyclobutanol **18** to give Pd(II)-alkoxide **31** which, following β-carbon elimination, would yield Pd(II)-alkyl intermediate **32**. Finally, reductive elimination would forge the cross-coupled adduct and regenerate the Pd(0) catalyst. For the formation of the undesired coupling product (**29**), we hypothesized that instead of undergoing the desired reductive elimination, complex **32** undergoes competing β-hydride elimination to give Pd(II)-hydride **33** and cyclohexanone **34** (Figure 4C). Re-addition of the Pd(II)-hydride across the exo-methylene of **34** leads to Pd(II)-alkyl complex **35**—the C1 epimer of complex **32**—which, upon undergoing reductive elimination, produces undesired diastereomer **29** and regenerates the Pd(0) catalyst.

On the basis of this proposed mechanism, we hypothesized that tuning the electronics of the Pd complex by modifying the ligands and additives could make the reductive elimination pathway of Pd(II)-alkyl species **32** more favorable over the undesired β-hydride elimination pathway. Specifically, we envisioned that decreasing the electron density on the Pd center would increase the rate of reductive elimination leading to the desired cross-coupled product (**28**).[47] In accordance with this hypothesis, we found the ligand $AsPh_3$ capable of providing the desired diastereomer (**28**), albeit in a low 8% yield and with poor diastereoselectivity (Figure 4A, entry 2). An NOE correlation between protons at the C1 and C17 positions confirmed the identity and relative stereochemistry of this product. The improved yield of desired diastereomer **28** obtained with $AsPh_3$ is believed to result from the weaker sigma donor ability of $AsPh_3$ compared to phosphine ligands like SPhos.[48,49] Consistent with generating an electron-deficient palladium complex, trials employing $AsPh_3$ proceeded in low overall conversion, presumably due to slower oxidative addition. However, this lower rate was addressed by increasing the catalyst loading (entry 3), which resulted in higher levels of conversion to both **28** (20% yield) and **29** (45% yield). Satisfied with the overall conversion of the reaction, we returned to improving the diastereoselectivity by screening additives. Recent studies have highlighted the effectiveness of electron-deficient olefins in promoting reductive elimination over competing β-hydride elimination.[47,50] The addition of 1,4-benzoquinone has been previously demonstrated to exhibit this effect,[51–53] and in our case led to a remarkable improvement in diastereoselectivity, providing the desired diastereomer in 67% yield and the undesired diastereomer in only 5% yield (entry 4). These optimal conditions proved to be highly scalable, giving the desired product in a comparable 68% yield on gram scale with respect to the C-ring fragment (entry 5). Having successfully assembled the A/C ring system of the taxane framework by coupling two carvone-derived fragments, we turned our attention to constructing the central eight-membered B-ring and completing our synthesis of diverse taxane cores.

Synthesis of Diverse Taxane Cores.

Beginning with the synthesis of the taxagifine core (**16**, Figure 5), cross-coupled adduct **28** was subjected to a two-step sequence involving methyl lithium addition into the aldehyde, followed by DMP oxidation of the resulting hydroxy group to afford diketone **36** in 47% yield over two steps. Enolization of the northern ketone group of **36** using LHMDS resulted in an intramolecular aldol cyclization which proceeded smoothly at room temperature to construct the eight-membered B-ring in 85% yield, thus completing the 6/8/6 core (**37**) of the taxanes. Notably, all the steps up to this point were performed on gram scale. Taxagifine core **16** was then obtained following acid-mediated cleavage of the ketal to unveil the C13 ketone, and the structure of **16** was unambiguously confirmed through X-ray crystallographic analysis.[54] While this ketal cleavage step only proceeded in 33% yield, we observed high mass recovery (65% recovered **37**). Unfortunately, the use of more strongly acidic conditions (e.g., 15% HCl) resulted in cleavage of both the ketal and TBS ether moieties. Furthermore, extending the reaction time of the PPTS-mediated cleavage from 24 to 72 h resulted in a higher yield of **16** (48% yield), but with a lower recovery of the starting material (12% recovered **37**) due to the formation of several side products, including the ketal/TBS-cleaved product (S3, Supporting Information, page S19). With **16** in hand, we envisioned that one-electron reduction of the C13 carbonyl using SmI_2 would promote cleavage of the adjacent C12–O bond, thus setting the stage for accessing other taxane scaffolds. Indeed, we found that treatment of **16** with SmI_2 and LiBr led to the formation of the taxezopidine A core (**15**) in 63% yield. Additives are known to play a crucial role in modulating SmI_2 reactivity, and in our case, LiBr proved vital to delivering higher yields of product (Table S2, Supporting Information, page S20).[55,56] Notably, these conditions accomplished several transformations in a single step, including rearrangement of the C17–C12 oxo-bridge resident in **16** to the C17–C13 oxo-bridge of **15**, as well as elimination of the C11 hydroxy group with concomitant formation of the C11–C12 alkene group required for the downstream [2 + 2] cycloaddition.

Having intercepted the taxezopidine A core (**15**), we shifted focus to deoxygenating the C17 position to forge the *gem*-dimethyl motif characteristic of the taxol core (**14**). Invoking the keto-alcohol form of **15**, we first attempted a deoxygenation of the C17 primary hydroxy group using Myers' protocol;[57] however, no conversion was observed under these conditions. The stability of this hydroxy group to direct reduction—potentially due to the equilibrium favoring the hemiketal form—prompted us to first convert the hydroxy group to an alkyl iodide, followed by reduction of the C17–I bond. An Appel-type iodination of **15** led to the desired alkyl iodide (**38**) in an excellent 93% yield. At this stage we investigated several reducing conditions to complete our synthesis of the taxol core (**14**). Radical-based conditions (e.g., AIBN and Bu_3SnH) led to complex reaction mixtures with no discernible product formation. Similar outcomes were observed with the hydride sources $NaBH_4$ and $LiEt_3BH$. During our studies, a report by Townsend and co-workers identified $NaBH_3CN$ to be effective at reducing primary alkyl iodides.[58] Applying analogous conditions ($NaBH_3CN$, DMF, 100 °C) to our case also proved beneficial, delivering the taxol core (**14**)—confirmed by X-ray crystallographic analysis—in 72% yield. Under these reaction conditions, a rearranged 5/8/6 taxane core (**39**) was obtained as a side product in 14% yield. This latter scaffold is believed to arise through a Dowd–Beckwith rearrangement[59] initiated by

homolysis of the C17–I bond (Supporting Information, page S25). Reduction at a lower temperature (80 °C) was investigated as a potential solution to prevent this side reaction; however, this trial resulted in low conversion, producing a 2:1 mixture of recovered starting material to product.

With all three of our targeted classical taxane cores assembled, we set our sights on applying the key bioinspired transannular [2 + 2] photocycloaddition to construct the highly caged nonclassical cyclotaxane core (**13**). It is proposed that, biosynthetically, this type of cycloaddition forges the cyclobutane motif embedded in **4** and **5** from similar, albeit slightly more oxidized, precursors compared to **14**.[60,61] Nonetheless, we envisioned that taxol core **14** would serve as an effective model substrate—in lieu of a more oxidized skeleton—to probe the feasibility of this reaction. We were pleased to find that with simple blue LED irradiation (centered at ~460 nm) at room temperature, the taxol core readily underwent the desired cycloaddition to deliver the cyclotaxane core (**13**) in a remarkable 98% yield. Alternatively, we found that this cycloadduct could be obtained directly from alkyl iodide **38** using slightly modified conditions to promote a tandem deiodination/[2 + 2] cycloaddition. Unsurprisingly, however, this route led to a lower yield of **13** (48%) due to the formation of side products (**39** and **40**) that arise through radical-mediated pathways (Supporting Information, pages S25 and S29). Notably, visible light-induced [2 + 2] photocycloadditions are usually facilitated by an additive,[62] such as a photocatalyst.[63] This work, however, serves as a rare example of a [2 + 2] cycloaddition proceeding readily under just blue LED irradiation without any special additives.[64] To the best of our knowledge, this report also provides the first experimental evidence supporting the plausibility of this key biosynthetic step.[65]

CONCLUSIONS

In summary, we have developed unified, enantiospecific, syntheses of four distinct taxane cores (**13–16**) belonging to different subsets of the taxane family. This first-of-its-kind synthetic approach was achieved through a strategy that merged skeletal remodeling with bioinspired elements. Building on the foundation of our previous studies, the taxane diterpenoid ring system was assembled in relatively short order by independently remodeling two carvone-derived cyclobutanols and then joining them together using a powerful C–C bond cleavage/cross-coupling/aldol sequence. This convergent approach, which forged the more oxidized taxagifine core (**16**) first, mitigated late-stage oxidation manipulations and enabled us to rapidly construct other classical taxane cores, including the taxezopidine A (**15**) and taxol (**14**) cores. Notably, a Sm(II)-mediated rearrangement expedited this process. Finally, by leveraging bioinspired logic, the taxol core (**14**) was transformed into the nonclassical cyclotaxane core (**13**) using an unprecedented visible light-induced transannular [2 + 2] photocycloaddition. Together, these powerful tactics facilitated entry into multiple complex taxane cores, requiring only 13–16 steps from known materials. Given that over half of all known taxanes contain the four cores (**13–16**) presented here, this general synthetic approach may provide access to myriad taxane natural products and will serve as the foundation for future synthetic efforts.

Supplementary Material

Refer to Web version on PubMed Central for supplementary material.

ACKNOWLEDGMENTS

We are grateful to the United States National Institute of General Medical Sciences (NIGMS R35 GM130345) for financial support. M.A.P. and B.W. thank the NSF GRFP for graduate research fellowships (DGE 1106400 and 1752814). M.A.P. is grateful to the National Institute of General Medical Sciences for a predoctoral fellowship (F31GM139368). B.C.W. was supported by the Swiss National Science Foundation (SNSF) (P2BEP2_165400). J.S.H. is grateful to SK Innovations for a graduate training fellowship. N.R.O. was supported by a Ruth L. Kirschstein F32 postdoctoral fellowship through the National Institute of General Medical Sciences (F32GM123601). S.N. is grateful to the Naito Foundation for a postdoctoral fellowship. J.M.N. thanks the University of California for a UC LEADS research fellowship. We thank Dr. Hasan Celik (UC Berkeley College of Chemistry NMR facility) and Dr. Jeffrey Pelton (UC Berkeley QB3 NMR facility) for assistance with NMR experiments, Dr. Nicholas Settineri (UC Berkeley) for assistance with single-crystal X-ray diffraction studies, and Dr. Ulla Anderson (UC Berkeley) and Dr. Miao Zhang (UC Berkeley) for assistance with gathering HRMS data. Instruments in the College of Chemistry NMR facility are supported in part by NIH S10OD024998 and funds for the QB3 900 MHz NMR spectrometer were provided by the NIH through grant GM68933. We also thank Dr. Justin Jurczyk (UC Berkeley) and Dr. Christina Na (UC Berkeley) for assistance with data procurement.

REFERENCES

(1). Wang Y-F; Shi Q-W; Dong M; Kiyota H; Gu Y-C; Cong B Natural Taxanes: Developments Since 1828. Chem. Rev 2011, 111, 7652–7709. [PubMed: 21970550]

(2). Shigemori H; Kobayashi J Biological Activity and Chemistry of Taxoids from the Japanese Yew, Taxus cuspidata. J. Nat. Prod 2004, 67, 245–256. [PubMed: 14987066]

(3). Weaver BA How Taxol/Paclitaxel Kills Cancer Cells. Mol. Biol. Cell 2014, 25, 2677–2681. [PubMed: 25213191]

(4). Schneider F; Pan L; Ottenbruch M; List T; Gaich T The Chemistry of Nonclassical Taxane Diterpene. Acc. Chem. Res 2021, 54, 2347–2360. [PubMed: 33942612]

(5). Nicolaou KC; Yang Z; Liu JJ; Ueno H; Nantermet PG; Guy RK; Claiborne CF; Renaud J; Couladouros EA; Paulvannan K; Sorensen E Total synthesis of taxol. Nature 1994, 367, 630–634. [PubMed: 7906395]

(6). Holton RA; Somoza C; Kim MB; Liang F; Biediger RJ; Boatman PD; Shindo M; Smith CC; Kim S First Total Synthesis of Taxol. 1. Functionalization of the B Ring. J. Am. Chem. Soc 1994, 116, 1597–1598.

(7). Holton R; Kim MB; Somoza C; Liang F; Biediger R; Boatman PD; Shindo M; Smith CC; Kim S First Total Synthesis of Taxol. 2. Completion of the C and D Rings. J. Am. Chem. Soc 1994, 116, 1599–1600.

(8). Danishefsky SJ; Masters JJ; Young WB; Link JT; Snyder LB; Magee TV; Jung DK; Isaacs RCA; Bornmann WG; Alaimo CA; Coburn CA; Di Grandi MJ Total Synthesis of Baccatin III and Taxol. J. Am. Chem. Soc 1996, 118, 2843–2859.

(9). Wender PA; Badham NF; Conway SP; Floreancig PE; Glass TE; Gränicher C; Houze JB; Jänichen J; Lee D; Marquess DG; McGrane PL; Meng W; Mucciaro TP; Mühlebach M; Natchus MG; Paulsen H; Rawlins DB; Satkofsky J; Shuker AJ; Sutton JC; Taylor RE; Tomooka K The Pinene Path to Taxanes. 5. Stereocontrolled Synthesis of a Versatile Taxane Precursor. J. Am. Chem. Soc 1997, 119, 2755–2756.

(10). Wender PA; Badham NF; Conway SP; Floreancig PE; Glass TE; Houze JB; Krauss NE; Lee D; Marquess DG; McGrane PL; Meng W; Natchus MG; Shuker AJ; Sutton JC; Taylor RE The Pinene Path to Taxanes. 6. A Concise Stereocontrolled Synthesis of Taxol. J. Am. Chem. Soc 1997, 119, 2757–2758.

(11). Morihira K; Hara R; Kawahara S; Nishimori T; Nakamura N; Kusama H; Kuwajima I Enantioselective Total Synthesis of Taxol. J. Am. Chem. Soc 1998, 120, 12980–12981.

(12). Mukaiyama T; Shiina I; Iwadare H; Saitoh M; Nishimura T; Ohkawa N; Sakoh H; Nishimura K; Tani Y; Hasegawa M; Yamada K; Saitoh K Asymmetric Total Synthesis of Taxol\R. Chem.—Eur. J 1999, 5, 121–161.

(13). Doi T; Fuse S; Miyamoto S; Nakai K; Sasuga D; Takahashi T A Formal Total Synthesis of Taxol Aided by an Automated Synthesizer. Chem.—Asian J 2006, 1, 370–383. [PubMed: 17441074]

(14). Fukaya K; Tanaka Y; Sato AC; Kodama K; Yamazaki H; Ishimoto T; Nozaki Y; Iwaki YM; Yuki Y; Umei K; Sugai T; Yamaguchi Y; Watanabe A; Oishi T; Sato T; Chida N Synthesis of Paclitaxel. 1. Synthesis of the ABC Ring of Paclitaxel by SmI2-Mediated Cyclization. Org. Lett 2015, 17, 2570–2573. [PubMed: 26010812]

(15). Fukaya K; Kodama K; Tanaka Y; Yamazaki H; Sugai T; Yamaguchi Y; Watanabe A; Oishi T; Sato T; Chida N Synthesis of Paclitaxel. 2. Construction of the ABCD Ring and Formal Synthesis. Org. Lett 2015, 17, 2574–2577. [PubMed: 26010999]

(16). Hirai S; Utsugi M; Iwamoto M; Nakada M Formal Total Synthesis of (–)-Taxol through Pd-Catalyzed Eight-Membered Carbocyclic Ring Formation. Chem.—Eur. J 2015, 21, 355–359. [PubMed: 25346263]

(17). Kanda Y; Nakamura H; Umemiya S; Puthukanoori RK; Murthy Appala VR; Gaddamanugu GK; Paraselli BR; Baran PS Two-Phase Synthesis of Taxol. J. Am. Chem. Soc 2020, 142, 10526–10533. [PubMed: 32406238]

(18). Hu Y-J; Gu C-C; Wang X-F; Min L; Li C-C Asymmetric Total Synthesis of Taxol. J. Am. Chem. Soc 2021, 143, 17862–17870. [PubMed: 34641680]

(19). Iiyama S; Fukaya K; Yamaguchi Y; Watanabe A; Yamamoto H; Mochizuki S; Saio R; Noguchi T; Oishi T; Sato T; Chida N Total Synthesis of Paclitaxel. Org. Lett 2022, 24, 202–206. [PubMed: 34904840]

(20). Schneider F; Samarin K; Zanella S; Gaich T Total Synthesis of the Complex Taxane Diterpene Canataxpropellane. Science 2020, 367, 676–681. [PubMed: 32029626]

(21). Orr GA; Verdier-Pinard P; McDaid H; Horwitz SB Mechanisms of Taxol Resistance Related to Microtubules. Oncogene 2003, 22, 7280–7295. [PubMed: 14576838]

(22). Ferlini C; Raspaglio G; Mozzetti S; Cicchillitti L; Filippetti F; Gallo D; Fattorusso C; Campiani G; Scambia G The Seco-Taxane IDN5390 Is Able to Target Class III β-Tubulin and to Overcome Paclitaxel Resistance. Cancer Res. 2005, 65, 2397–2405. [PubMed: 15781655]

(23). Bernabeu E; Cagel M; Lagomarsino E; Moretton M; Chiappetta DA Paclitaxel: What Has Been Done and the Challenges Remain Ahead. Int. J. Pharm 2017, 526, 474–495. [PubMed: 28501439]

(24). Ojima I; Wang X; Jing Y; Wang C Quest for Efficacious Next-Generation Taxoid Anticancer Agents and Their Tumor-Targeted Delivery. J. Nat. Prod 2018, 81, 703–721. [PubMed: 29468872]

(25). Mendoza A; Ishihara Y; Baran PS Scalable Enantioselective Total Synthesis of Taxanes. Nat. Chem 2012, 4, 21–25.

(26). Brill ZG; Condakes ML; Ting CP; Maimone TJ Navigating the Chiral Pool in the Total Synthesis of Complex Terpene Natural Products. Chem. Rev 2017, 117, 11753–11795. [PubMed: 28293944]

(27). Masarwa A; Weber M; Sarpong R Selective C-C and C-H Bond Activation/Cleavage of Pinene Derivatives: Synthesis of Enantiopure Cyclohexenone Scaffolds and Mechanistic Insights. J. Am. Chem. Soc 2015, 137, 6327–6334. [PubMed: 25892479]

(28). Weber M; Owens K; Masarwa A; Sarpong R Construction of Enantiopure Taxoid and Natural Product-like Scaffolds Using a C-C Bond Cleavage/Arylation Reaction. Org. Lett 2015, 17, 5432–5435. [PubMed: 26485318]

(29). Lusi RF; Perea MA; Sarpong R C-C Bond Cleavage of α-Pinene Derivatives Prepared from Carvone as a General Strategy for Complex Molecule Synthesis. Acc. Chem. Res 2022, 55, 746–758. [PubMed: 35170951]

(30). Kuroda Y; Nicacio KJ; da Silva IA Jr; Leger PR; Chang S; Gubiani JR; Deflon VM; Nagashima N; Rode A; Blackford K; Ferreira AG; Sette LD; Williams DE; Andersen RJ; Jancar S; Berlinck RGS; Sarpong R Isolation, synthesis and bioactivity studies of phomactin terpenoids. Nat. Chem 2018, 10, 938–945. [PubMed: 30061613]

(31). Kerschgens I; Rovira AR; Sarpong R Total Synthesis of (–)-Xishacorene B from (R)-Carvone Using a C-C Activation Strategy. J. Am. Chem. Soc 2018, 140, 9810–9813. [PubMed: 30032603]

(32). Bermejo FA; Fernández Mateos A; Marcos Escribano A; Martín Lago R; Mateos Burón L; Rodríguez López M; Rubio González R Ti(III)-Promoted Cyclizations. Application to the Synthesis of (E)-endo-bergamoten-12-oic acids. Moth Oviposition Stimulants Isolated from Lycopersicon hirsutum. Tetrahedron 2006, 62, 8933–8942.

(33). Wang B; Perea MA; Sarpong R Transition Metal-Mediated C–C Single Bond Cleavage: Making the Cut in Total Synthesis. Angew. Chem., Int. Ed 2020, 59, 18898–18919.

(34). Matsumura S; Maeda Y; Nishimura T; Uemura S Palladium-Catalyzed Asymmetric Arylation, Vinylation, and Allenylation of tert-Cyclobutanols via Enantioselective C–C Bond Cleavage. J. Am. Chem. Soc 2003, 125, 8862–8869. [PubMed: 12862483]

(35). Nicolaou KC; Ellery SP; Chen JS Samarium Diiodide Mediated Reactions in Total Synthesis. Angew. Chem., Int. Ed 2009, 48, 7140–7165.

(36). Renata H; Zhou Q; Baran PS Strategic Redox Relay Enables A Scalable Synthesis of Ouabagenin, A Bioactive Cardenolide. Science 2013, 339, 59–63. [PubMed: 23288535]

(37). Lusi RF; Sennari G; Sarpong R Total Synthesis of Nine Longiborneol Sesquiterpenoids Using a Functionalized Camphor Strategy. Nat. Chem 2022, 14, 450–456. [PubMed: 35165424]

(38). Newhouse T; Baran PS If C–H Bonds Could Talk: Selective C–H Bond Oxidation. Angew. Chem., Int. Ed 2011, 50, 3362–3374.

(39). Nishimura T; Ohe K; Uemura S Oxidative Transformation of Tert-Cyclobutanols by Palladium Catalysis under Oxygen Atmosphere. J. Org. Chem 2001, 66, 1455–1465. [PubMed: 11312980]

(40). Pappo R; Allen D Jr; Lemieux R; Johnson W Notes - Osmium Tetroxide-Catalyzed Periodate Oxidation of Olefinic Bonds. J. Org. Chem 1956, 21, 478–479.

(41). Yu W; Mei Y; Kang Y; Hua Z; Jin Z Improved Procedure for the Oxidative Cleavage of Olefins by OsO4–NaIO4. Org. Lett 2004, 6, 3217–3219. [PubMed: 15355016]

(42). Evans DA; Chapman KT; Carreira EM Directed reduction of. beta.-hydroxy ketones employing tetramethylammonium triacetoxyborohydride. J. Am. Chem. Soc 1988, 110, 3560–3578.

(43). Saksena AK; Mangiaracina P Recent Studies on Veratrum Alkaloids: A New Reaction of Sodium Triacetoxyborohydride [NaBH(OAc)3]. Tetrahedron Lett. 1983, 24, 273–276.

(44). De Mico A; Margarita R; Parlanti L; Vescovi A; Piancatelli G A Versatile and Highly Selective Hypervalent Iodine (III)/2,2,6,6-Tetramethyl-1-Piperidinyloxyl-Mediated Oxidation of Alcohols to Carbonyl Compounds. J. Org. Chem 1997, 62, 6974–6977.

(45). Dess DB; Martin JC Readily Accessible 12-I-5 Oxidant for the Conversion of Primary and Secondary Alcohols to Aldehydes and Ketones. J. Org. Chem 1983, 48, 4155–4156.

(46). Tsunoda T; Suzuki M; Noyori R A Facile Procedure for Acetalization under Aprotic Conditions. Tetrahedron Lett. 1980, 21, 1357–1358.

(47). Johnson JB; Rovis T More than Bystanders: The Effect of Olefins on Transition-Metal-Catalyzed Cross-Coupling Reactions. Angew. Chem., Int. Ed 2008, 47, 840–871.

(48). Farina V; Krishnan B Large Rate Accelerations in the Stille Reaction with Tri-2-furylphosphine and Triphenylarsine as Palladium Ligands: Mechanistic and Synthetic Implications. J. Am. Chem. Soc 1991, 113, 9585–9595.

(49). Otto S; Roodt A Quantifying the electronic cis effect of phosphine, arsine and stibine ligands by use of rhodium(I) Vaska-type complexes. Inorg. Chim. Acta 2004, 357, 1–10.

(50). Estrada JG; Williams WL; Ting SI; Doyle AG Role of Electron-Deficient Olefin Ligands in a Ni-Catalyzed Aziridine Cross-Coupling to Generate Quaternary Carbons. J. Am. Chem. Soc 2020, 142, 8928–8937. [PubMed: 32348673]

(51). Willcox D; Chappell BGN; Hogg KF; Calleja J; Smalley AP; Gaunt MJ A general catalytic β-C-H carbonylation of aliphatic amines to β-lactams. Science 2016, 354, 851–857. [PubMed: 27856900]

(52). Hull KL; Sanford MS Mechanism of Benzoquinone-Promoted Palladium-Catalyzed Oxidative Cross-Coupling Reactions. J. Am. Chem. Soc 2009, 131, 9651–9653. [PubMed: 19569623]

(53). Sköld C; Kleimark J; Trejos A; Odell LR; Nilsson Lill SO; Norrby P-O; Larhed M Transmetallation Versus β-Hydride Elimination: The Role of 1,4-Benzoquinone in Chelation-

Controlled Arylation Reactions with Arylboronic Acids. Chem.—Eur. J 2012, 18, 4714–4722. [PubMed: 22374849]

(54). Legault CY; CYLview, 1.0b; Université de Sherbrooke, 2009, http://www.cylview.org (accessed March 14, 2022).

(55). Dahlén A; Hilmersson G Samarium (II) Iodide Mediated Reductions – Influence of Various Additives. Eur. J. Inorg. Chem 2004, 3393–3403.

(56). Cha JY; Yeoman JTS; Reisman SE A Concise Total Synthesis of (–)-Maoecrystal Z. J. Am. Chem. Soc 2011, 133, 14964–14967. [PubMed: 21877709]

(57). Myers AG; Movassaghi M; Zheng B Single-Step Process for the Reductive Deoxygenation of Unhindered Alcohols. J. Am. Chem. Soc 1997, 119, 8572–8573.

(58). Nguyen JM; Townsend SD Total Synthesis of the Photorhabdus temperata ssp. Cinereal 3240 Zwitterionic Trisaccharide Repeating Unit. Unit. Org. Lett 2021, 23, 5922–5926. [PubMed: 34314177]

(59). Dowd P; Zhang W Free Radical-Mediated Ring Expansion and Related Annulations. Chem. Rev 1993, 93, 2091–2115.

(60). Huo C-H; Su X-H; Wang Y-F; Zhang X-P; Shi Q-W; Kiyota H Canataxpropellane, a Novel Taxane with a Unique Polycyclic Carbon Skeleton (Tricyclotaxane) from the Needles of Taxus Canadensis. Tetrahedron Lett. 2007, 48, 2721–2724.

(61). Zhang M-L; Dong M; Huo C-H; Li L-G; Sauriol F; Shi Q-W; Gu Y-C; Makabe H; Kiyota H Taxpropellane: A Novel Taxane with an Unprecedented Polycyclic Skeleton from the Needles ofTaxus canadensis. Eur. J. Org. Chem 2008, 5414–5417.

(62). Poplata S; Tröster A; Zou Y-Q; Bach T Recent Advances in the Synthesis of Cyclobutanes by Olefin [2 + 2] Photocycloaddition Reactions. Chem. Rev 2016, 116, 9748–9815. [PubMed: 27018601]

(63). Du J; Skubi KL; Schultz DM; Yoon TP A Dual-Catalysis Approach to Enantioselective [2 + 2] Photocycloadditions Using Visible Light. Science 2014, 344, 392–396. [PubMed: 24763585]

(64). Some examples of visible-light induced [2 + 2] photocycloadditions that do not require special additives are provided in ref 62. One specific example includes:Christl M; Braun M; Deeg O; Wolff S Photochemical Reactions of Chloranil with Cyclooctene, 1,5-Cyclooctadiene, and Cyclohexene Revisited. Eur. J. Org. Chem 2011, 968–982.

(65). This type of bioinspired transannular [2 + 2] photocycloaddition has also been observed by the Gaich group in their studies which we are aware of through personal communication with Prof. Tanja Gaich.

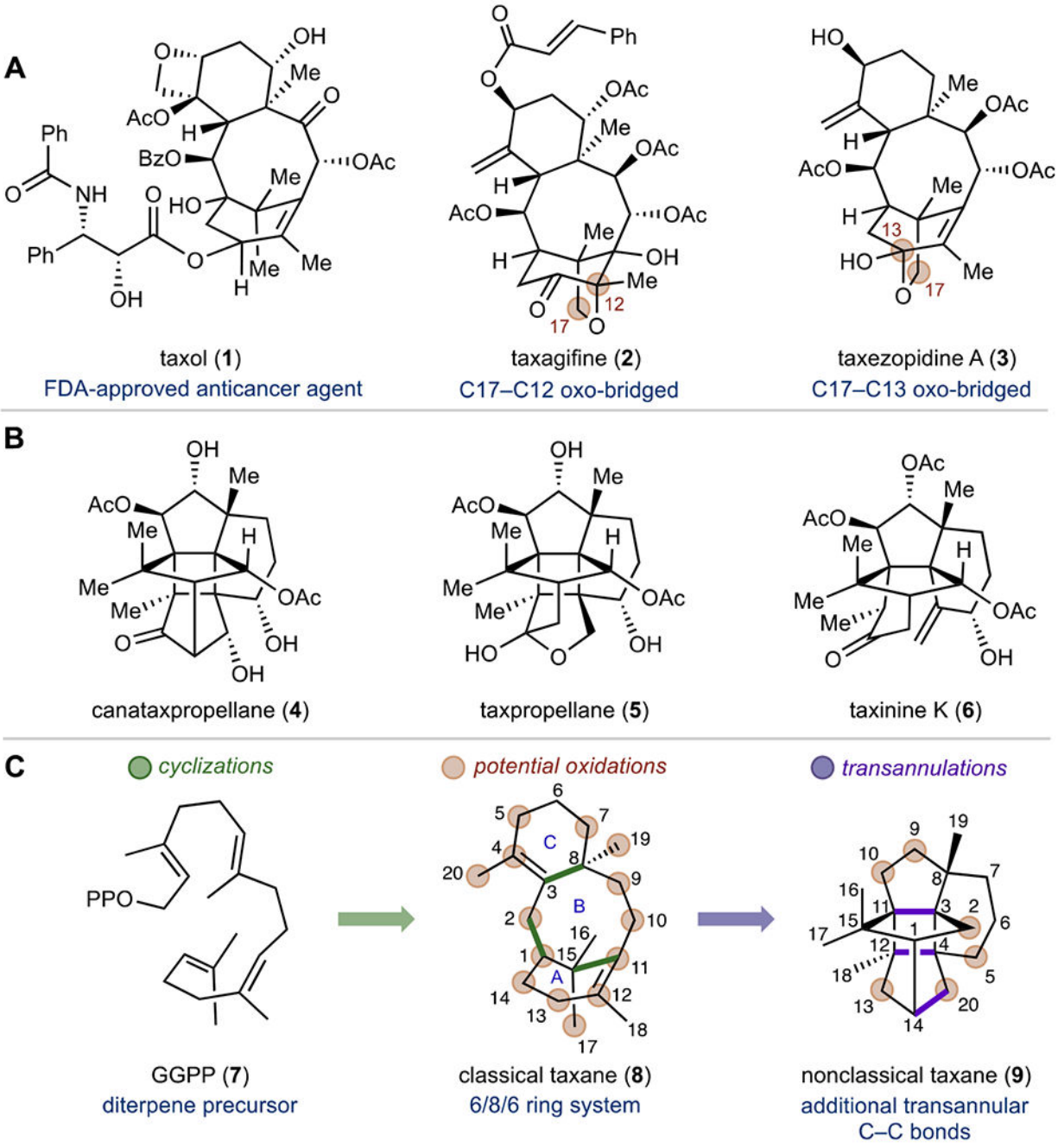

Figure 1.

Taxane natural products. (A) Representative classical taxanes contain a 6/8/6 ring system decorated with varying patterns of oxygenation. (B) Representative nonclassical cyclotaxanes contain the classical 6/8/6 core with additional transannular bonds. (C) Proposed taxane biosynthesis.

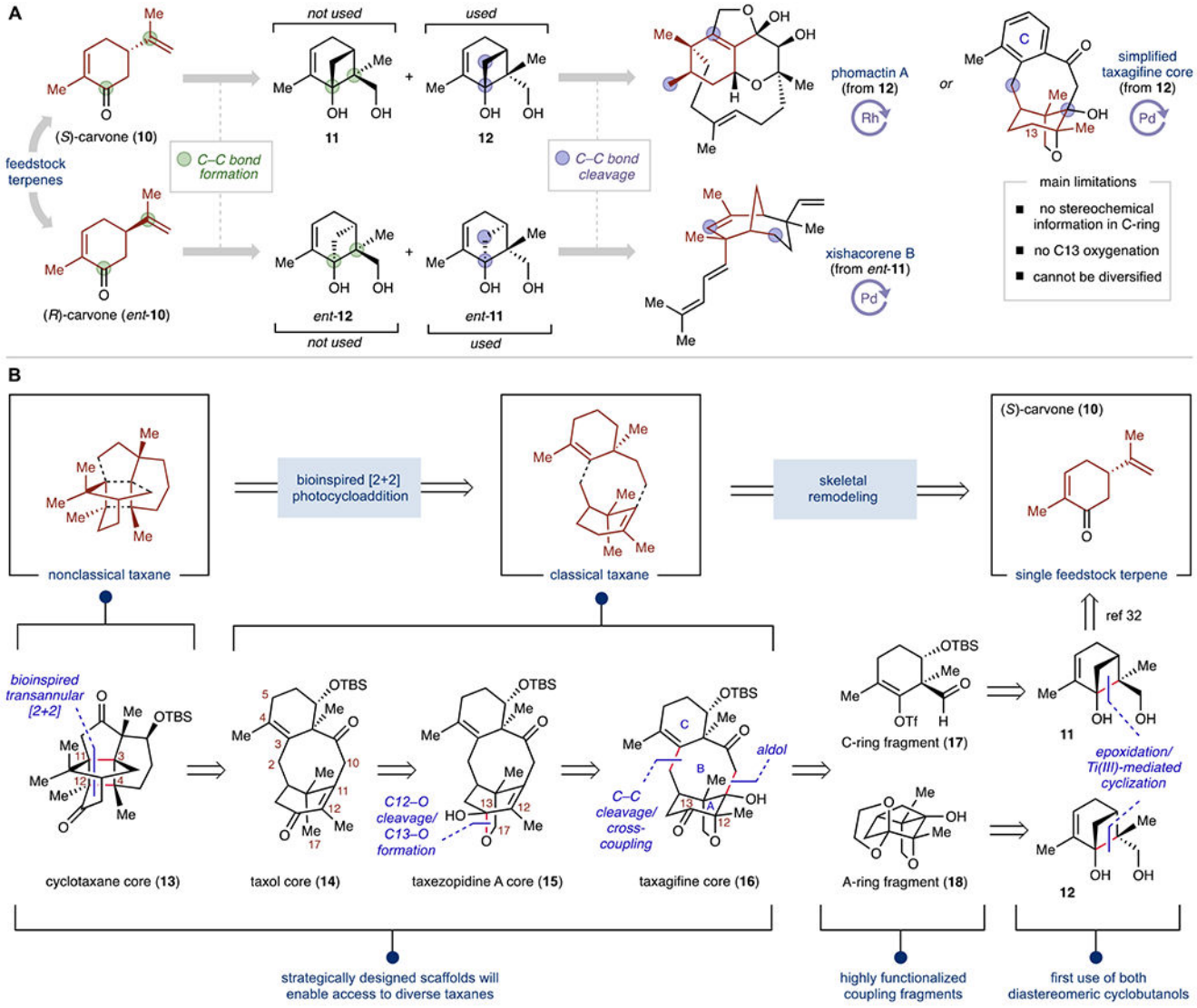

Figure 2.

Carvone skeletal remodeling strategy for complex diterpenoid synthesis. (A) Our previous syntheses of phomactin A, xishacorene B, and a simplified taxane core. One carvone-derived cyclobutanol was remodeled to each of these scaffolds using transition metal-catalyzed C–C bond cleavage. (B) Our current approach to taxane synthesis. A series of nonclassical and classical taxane cores were envisioned to arise from both carvone-derived cyclobutanols by using bioinspired tactics and skeletal remodeling enabled by C–C and C–O bond cleavage.

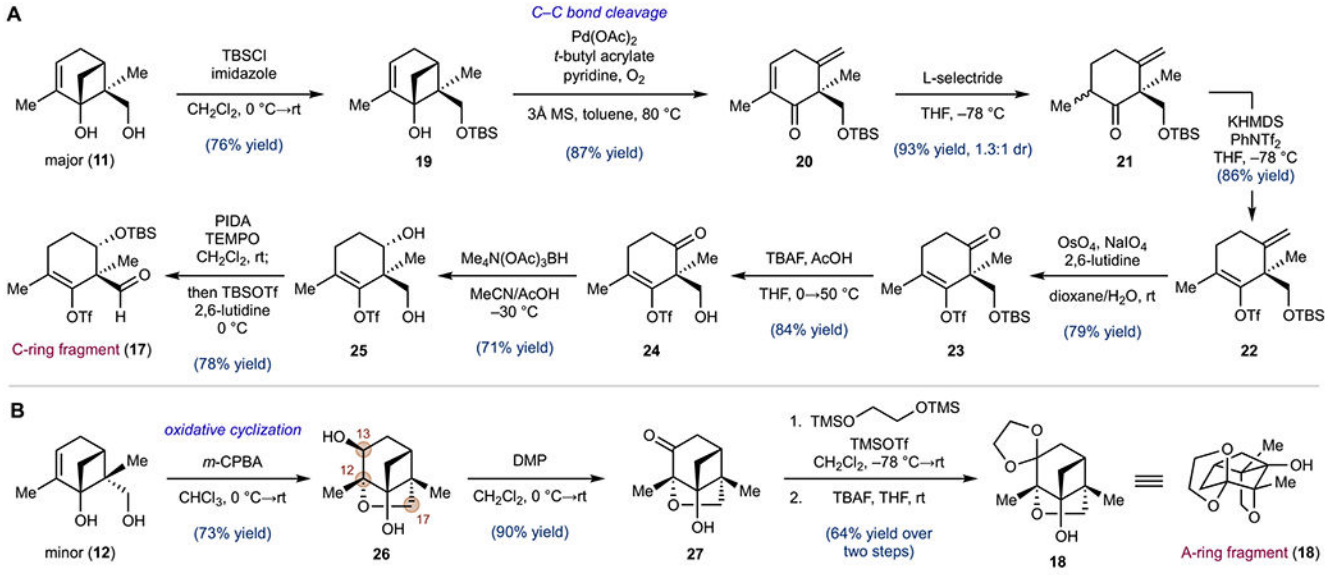

Figure 3.

Synthesis of the coupling fragments. (A) Synthetic route to the northern C-ring fragment (**17**). (B) Synthetic route to the southern A-ring fragment (**18**). All steps leading to both these fragments were performed on gram scale. TBSCl, *tert*-butyldimethylsilyl chloride; MS, molecular sieves; THF, tetrahydrofuran; KHMDS, potassium bis(trimethylsilyl)amide; $PhNTf_2$, phenyl triflimide; TBAF, tetrabutylammonium fluoride; PIDA, (diacetoxyiodo)benzene; TEMPO, 2,2,6,6-tetramethylpiperidine 1-oxyl; TBSOTf, *tert*-butyldimethylsilyl trifluoromethanesulfonate; *m*-CPBA, *meta*-chloroperbenzoic acid; DMP, Dess–Martin periodinane; TMSOTf, trimethylsilyl trifluoromethanesulfonate.

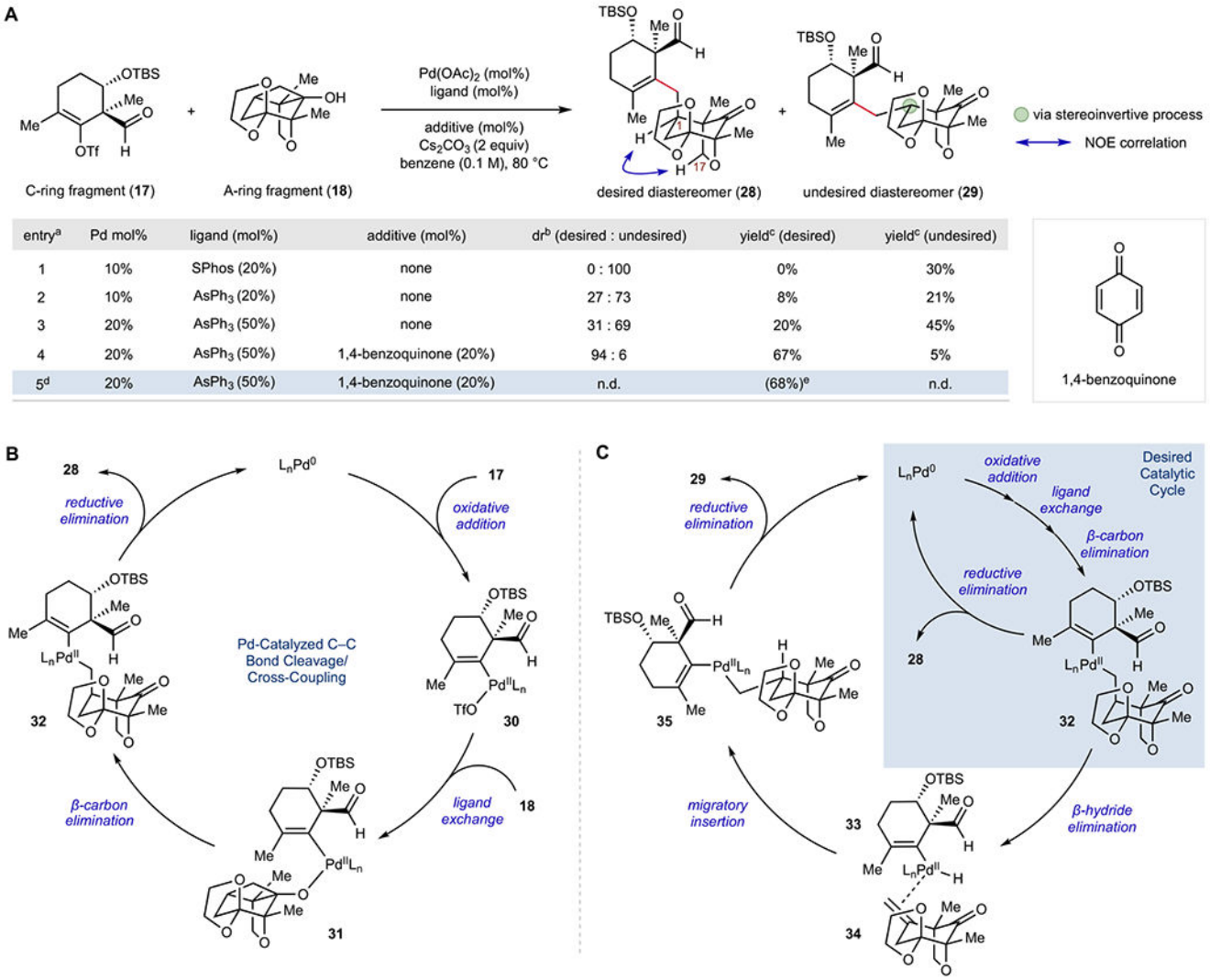

entry[a]	Pd mol%	ligand (mol%)	additive (mol%)	dr[b] (desired : undesired)	yield[c] (desired)	yield[c] (undesired)
1	10%	SPhos (20%)	none	0 : 100	0%	30%
2	10%	$AsPh_3$ (20%)	none	27 : 73	8%	21%
3	20%	$AsPh_3$ (50%)	none	31 : 69	20%	45%
4	20%	$AsPh_3$ (50%)	1,4-benzoquinone (20%)	94 : 6	67%	5%
5[d]	20%	$AsPh_3$ (50%)	1,4-benzoquinone (20%)	n.d.	(68%)[e]	n.d.

Figure 4.

Pd-catalyzed C–C bond cleavage/cross-coupling. (A) Optimization of the cross-coupling reaction. (B) Proposed mechanism of the desired coupling. (C) Proposed mechanism of the undesired coupling. [a]All entries: $Pd(OAc)_2$ as pre-catalyst, ca. 0.02 mmol **18** (unless otherwise noted), 1.25 equiv **17**, 2 equiv Cs_2CO_3, 0.1 M (benzene), 80 °C, 21 h (unless otherwise noted). [b]dr determined from ^1H NMR of crude reaction mixture. [c]^1H NMR yield using mesitylene as an internal standard, based on the limiting coupling fragment (**18**). [d]2.9 mmol **18** and 27 h. [e]Isolated yield. A full summary of the cross-coupling optimization is provided in the Supporting Information (Table S1, page S14). SPhos, 2-dicyclohexylphosphino-2′,6′-dimethoxybiphenyl; NOE, nuclear Overhauser effect; n.d., not determined.

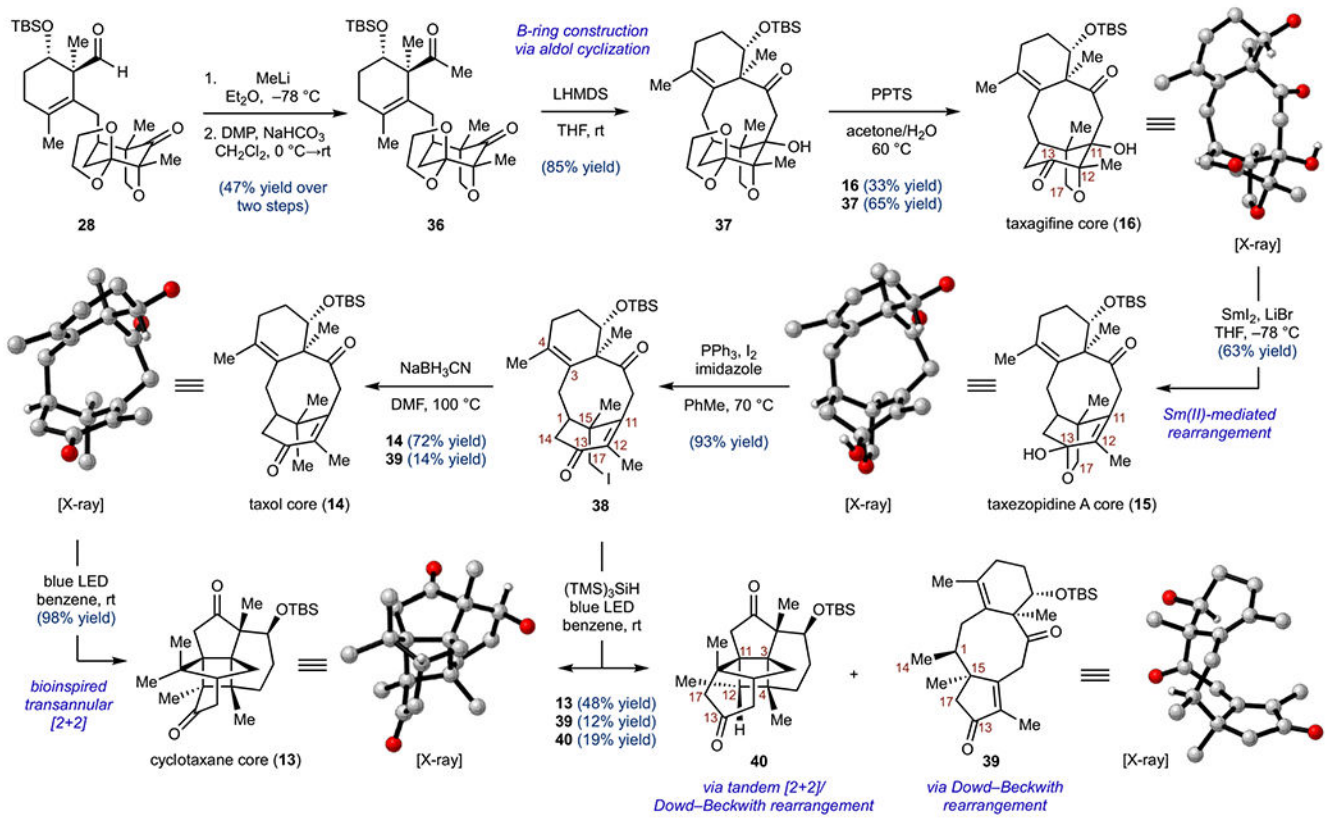

Figure 5.

Synthesis of diverse taxane cores. X-ray crystal structures were visualized using CYLview,[54] and all TBS groups and nonstereogenic hydrogens have been removed for clarity. LHMDS, lithium bis(trimethylsilyl)amide; PPTS, pyridinium *p*-toluenesulfonate; PhMe, toluene; DMF, dimethylformamide; $(TMS)_3SiH$, tris(trimethylsilyl)silane.